IJBPAS, November, Special Issue, 2021, 10(11): 198-215
ISSN: 2277–4998

International Journal of Biology, Pharmacy and Allied Sciences (IJBPAS)
'A Bridge Between Laboratory and Reader'

www.ijbpas.com

CORROSION INHIBITION EFFECT OF 2-[(2-MERCAPTO-PHENYLIMINO) METHYL] BENZOIC ACID FOR MILD STEEL IN SIMULATED CONCRETE PORE SOLUTION

P.SELVI[1], S.VALARSELVAN[1*] AND S. S. SYED ABUTHAHIR[2]

1: PG and Research Department of Chemistry, H.H. The Rajah's College (Autonomous), Affiliated to Bharathidasan University, Pudukottai, Tamilnadu, India

2: PG and Research Department of Chemistry, Jamal Mohamed College (Autonomous), Affiliated to Bharathidasan University, Tiruchirappalli, Tamilnadu, India

***Corresponding Author: S.Valarselvan**; **E Mail:** svalarselvan@gmail.com

Received 19th July 2021; Revised 20th Aug. 2021; Accepted 29th Sept. 2021; Available online 1st Nov. 2021

https://doi.org/10.31032/IJBPAS/2021/10.11.1015

ABSTRACT

The corrosion inhibition effect of 2-[(2-mercapto-phenylimino) methyl] benzoic acid has been evaluated for mild steel is immersed in simulated concrete pore solution (SCPS) by weight loss method. The weight-loss method was used to calculate the inhibition efficiency and corrosion rate. The efficiency of corrosion inhibition increases as the content of an inhibitor, 2-[(2-mercapto-phenylimino) methyl] benzoic acid, increases. When the concentration of inhibitor is increased, the corrosion rate reduces. This is because a protective coating forms over the mild steel surface at greater concentrations of inhibitor solution, which inhibits the active site of mild steel from becoming active. The creation of a protective coating over the mild steel surface was confirmed using electrochemical measurements. FTIR was used to characterize the surface layer that developed over the mild steel surface. Surface analysis techniques such as scanning electron microscopy can also detect it. SEM was used to examine the smoothness and roughness of mild steel surfaces such as polished, corroded, and inhibitor systems.

Keywords: **Corrosion, FTIR, Mild steel, Weight loss method and Scanning Electron Microscopy**

INTRODUCTION

Reinforced concrete is a common building material that contributes significantly to economic development **[1]**. The premature deterioration of reinforced concrete structures owing to reinforcing steel corrosion has cost modern society a significant amount of money. As a result, research on the corrosion behavior of reinforcing steel is quite useful **[2, 3]**. Because of the high alkalinity of the concrete pore solution, reinforcing steel in concrete can be protected from corrosion under normal conditions by producing a compact passive layer on the steel surface. By testing the steel in a concrete simulated pore solution, which is mostly made up of saturated calcium hydroxide ($Ca(OH_2)$), sodium hydroxide (NaOH), and potassium hydroxide, the long time required for chlorides to penetrate the concrete cover can be avoided (KOH). However, saturated $Ca(OH)_2$ has been utilized as a substitute for pore solution in various rebar corrosion investigations **[4]**. In addition, various ions in pore solution, particularly sodium and potassium, may play a role in passivation and corrosion processes. Corrosion researchers are interested in learning more about the process of Cl- causing steel depassivation and the threshold concentration for steel corrosion. The critical chloride concentrations were measured in a variety of ways due to variances in experimental settings, measuring methodologies, and other factors. Because of the complexity of reinforced concrete systems, simulated concrete pore solutions are often employed to research reinforcing steel corrosion behavior **[5]**, which helps understand the corrosion mechanism of reinforcing steel.

The corrosion behavior of metals in the presence of simulated concrete pore solution has been studied in several research studies **[6]**. In most cases, rebar has been used in such research. The primary goal of this research is to see how efficient 2-[(2-mercapto-phenylimino) methyl] benzoic acid is as a corrosion inhibitor for mild steel immersed in a simulated concrete pore solution. The weight-loss method was used to analyze the impact of the inhibitor on corrosion rate and inhibition efficiency. Electrochemical research such as alternating current impedance spectra and polarisation studies are used to determine the mechanistic features of corrosion inhibition. The Fourier Transform Infrared (FTIR) spectroscopy technique was used to evaluate the protective film that was generated over the surface of mild steel. Scanning Electron Microscopy

was used to determine the smoothness of mild steel when compared to polished mild steel, corroded mild steel (blank), and mild steel in an inhibitor system (SEM).

MATERIALS AND METHODS

Corrosion inhibition of mild steel in simulated concrete pore solution by 2-[(2-mercapto-phenylimino) methyl] benzoic acid has been studied.

Mild steel specimens Preparation

S-0.026%, P-0.06%, Mn-0.4%, C-0.1% and the rest ion were polished to mirrors finish and degreased with acetone and used for the weight loss method.

Simulated Concrete Pore Solution (SCPS)

In this work, the SCP solution is a saturated calcium hydroxide solution. The AC impedance spectra were acquired using an iron electrode immersed in SCP solution.

Preparation of stock solutions

Double distilled water was used wherever necessary in the preparation of solutions. Prepared 2-[(2-mercapto-phenylimino) methyl] benzoic acid is taken as such and they were diluted to the required concentration. The required concentration of the 2-[(2-mercapto-phenylimino) methyl] benzoic acid stock solution was prepared by dissolving the in a minimum amount of ethanol and making up to the desired volume with double distilled water. Then the required volume from the inhibitor stock solution was added to the SCP solution to obtain the desired concentration.

Weight loss method

Weight loss measurements were taken using the manner previously described **[7-8]**. The mild steel specimens were immersed in aqueous solution SCP without and with varying levels of inhibitor (50 ppm – 250 ppm) for 24 hours to determine weight loss. After elapsed time, the specimen was taken out, washed, dried and weighed accurately. The inhibition efficiency (IE %) was determined by the following equation.

$$\text{I.E. (\%)} = \frac{W_o - W_1}{W_o} \times 100$$

Where W_1 and W_o are the weight loss values in g in presence and absence of inhibitors, respectively.

Potentiodynamic polarization study

Polarization experiments were carried out with a three-electrode cell assembly in a H & CH electrochemical workstation impedance analyzer model CHI660A, Austin, USA. The working electrode was mild steel, with a continuous 1 cm2 area exposed on one face and the rest shielded by red lacquer. As the reference electrode, a saturated calomel electrode (SCE) was utilized, and the counter

electrode was a rectangular platinum foil. When compared to the area of the working electrode, the counter electrode had a substantially larger surface area. On the counter electrode, this can produce a homogeneous potential field. The findings were calculated, including Tafel slopes, Icorr, and Ecorr values **[9]**.

In the absence and presence of inhibitor, the working electrode and platinum electrode were submerged in an aqueous solution containing SCP. A salt bridge was used to link a saturated calomel electrode to the test solution. Plots of potential (E) vs. log current (I) were made. E Vs log I plots were used to evaluate the corrosion potential (E_{corr}) and Tafel slopes b_a, b_c..

AC impedance measurements

AC impedance studies were carried out in an H & CH electrochemical work station impedance analyzer model CHI660A , Austin, USA. The cell set up was the same as that used for polarization measurements. For the system to reach a steady state open circuit potential, a time interval of 5 to 10 minutes was given. An A.C. potential of 10 mV was then overlaid over this steady state potential. The frequency of the AC was altered between 100 KHz and 100 MHz. For various frequencies, the real part (z') and imaginary part (z'') of the cell impedance were measured in ohms. The R_t (charge transfer resistance) and C_{dl} (double layer capacitance) values were calculated. C_{dl} values were calculated using the following relationship **[10]**.

$$C_{dl} = \frac{1}{2 \times 3.14 \times R_t \times f_{max}}$$

Surface characterization studies

For one day, the mild steel specimens were immersed in both blank and inhibitor solutions. The specimens were taken out and dried after one day. Various analysis techniques were used to examine the nature of the film that formed on the surface of the carbon steel specimens.

Surface analysis by FTIR spectra

A Perkin Elmer Spectrum Version spectrophotometer was used to record FTIR spectra. The film was carefully removed, and the FTIR spectra were taken after it was thoroughly combined with KBr and formed into pellets.

The specimens were taken out of the test fluids and dried after a one-day immersion time in varied settings. The coating that had formed on the surface was carefully scratched and properly blended to ensure that it was consistent throughout **[11]**. A Perkin Elmer Spectra Version spectrophotometer was used to record the FTIR spectrum of the powder (KBr pellet).

Scanning Electron Microscopic studies (SEM)

SEM was used to examine the difference like metal surface before and after the metal surface is in direct contact with the corrodent solution and to observe the effect of the addition of the inhibitor **[12]**. Thus SEM was used to analyze the topography of the mild steel surface after corroding in the presence and absence of the inhibitor. The SEM image was taken by the SEM instrument, JEOL MODEL JSM 6390.

RESULTS

Results of weight loss method

The corrosion rates (CR) of mild steel immersed in an aqueous solution containing SCP and also inhibition efficiencies (IE) in the absence and presence of inhibitor 2-[(2-mercapto-phenylimino) methyl] benzoic acid obtained by weight loss method. The concentration of inhibitor, corrosion rate and inhibition efficiency values are given in **Table 1**.

Electrochemical methods

The electrochemical measurements encompass a way of calculating the rate of corrosion of carbon steel. It permits rapid evaluation of the performance of inhibitors, the durability of surface film and also the inhibition efficiency of corrosion inhibitors **[13]**.

The following techniques were used for mild steel corrosion in SCP in the absence and in the presence of the MPIMB inhibitor system to know whether they act as cathodic or anodic or mixed type inhibitors and also to formulate an appropriate mechanism for their inhibition action on the carbon steel corrosion.

Results of potentiodynamic polarization study

The creation of a protective coating on the carbon steel surface was investigated using polarization analysis. The linear polarization resistance values (LPR) increase as a protective coating is developed on the carbon steel surface, while the corrosion current value (Icorr) drops. **Figure 1** shows the potentiodynamic polarization curves of carbon steel immersed in an aqueous solution containing 60 ppm Cl- in the presence and absence of inhibitors. Table 2 contains the corrosion parameters.

Results of alternating current impedance spectra

The production of a protective coating on the mild steel surface has been confirmed using AC impedance spectra (electrochemical impedance spectra) **[14-15]**. Charge transfer resistance (R_t) increases, double layer capacitance value (C_{dl}) lowers,

and impedance log (z/ohm) value increases when a protective film is created on the mild steel surface **[16-17]**. **Figure 2 (a)** (Nyquist plots) and **Figure 3 (a, b)** illustrate the AC impedance spectra of carbon steel immersed in an aqueous solution containing SCP in the absence and presence of inhibitors (MPIMB) (Bode plots). **Table 3** shows the AC impedance parameters determined from Nyquist plots, namely charge transfer resistance (Rt) and double-layer capacitance (C_{dl}). **Table 3** also includes the impedance log (z/ohm) values generated from Bode plots.

FTIR spectral characterization

FTIR spectra have been used to analyze the protective film formed on the mild steel surface **[18]**. The structure of MPIMB is shown in **Figure 4**. The FTIR spectrum (KBr) of pure 2-[(2-mercapto-phenylimino) methyl] benzoic acid (MPIMB) is shown in Figure 5a and the values are in **Table 4**. The FTIR spectrum (KBr) of the film formed on the carbon steel surface after immersion in an aqueous solution containing SCP + 250 ppm of MPIMB is shown in Figure 5b and the values are in **Table 4**.

Surface characterization of mild steel by SEM

SEM study gives a surface morphology result to understand the nature of the surface layer in the presence and absence of corrosion inhibitors and the extent of corrosion of mild steel. The SEM images of the mild steel surface are studied. SEM provides a pictorial representation of the mild steel surface. To understand the nature of the layer formed in the absence and presence of 2-[(2-mercapto-phenylimino) methyl] benzoic acid inhibitor on the carbon steel surface and the extent of corrosion of mild steel, the SEM micrographs of the surface are examined. The SEM images of mild steel specimen immersed in SCP for 24 hours in the absence and presence of 2-[(2-mercapto-phenylimino) methyl] benzoic acid inhibitor system are shown in **Figure 6 (a, b & c)** respectively.

The mild steel specimen is immersed in the SCP solution containing inhibitor for 24 hrs. The specimen is taken out, dried and observed under the investigation of SEM. The images of fresh carbon steel is shown (control) in **Figure 6a**. The mild steel surface has been damaged due to metal dissolution in SCP is shown (blank) in **Figure 6b**. The mild steel surface dipped in SCP-containing inhibitor is shown in **Figure 6c**.

Table 1: Corrosion rates (CR) and inhibition efficiency (IE %) data obtained from weight loss measurements for mild steel is immersed in an aqueous solution containing SCP without and with various concentration of 2-[(2-mercapto-phenylimino) methyl] benzoic acid inhibitor

- **Inhibitor System: 2-[(2-mercapto-phenylimino) methyl] benzoic acid**
- **Immersion period: 24 hours**

Blank	MPIMB (ppm)	*CR* (mdd)	*IE* (%)
SCPS	0	67.10	----
	50	44.31	30
	100	34.52	44
	150	26.41	54
	200	19.10	68
	250	7.82	84

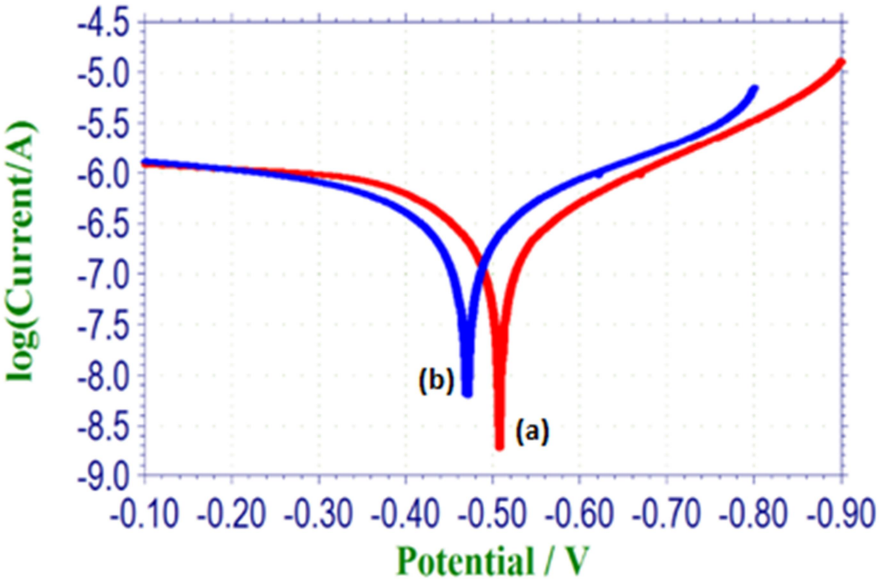

Figure 1: Potentiodynamic polarization curves for corrosion of mild steel in SCP in absence and presence of MPIMBinhibitor
(a) Mild steel in SCP (blank)
(b) Mild steel in SCP with 250 ppm of MPIMB

Table 2: Potentiodynamic Polarization parameters for the corrosion of mild steel in SCP for the aqueous solution of MPIMB system

Systems	E_{corr} vs SCE (mV)	I_{corr} (A/cm^2)	b_a (mV/dec)	b_c (mV/dec)	LPR (ohm cm^2)
SCP	- 508	2.443×10^{-7}	186	0.2060	1740
SCP + 250 ppm MPIMB	- 470	2.987×10^{-7}	195	0.2444	1783

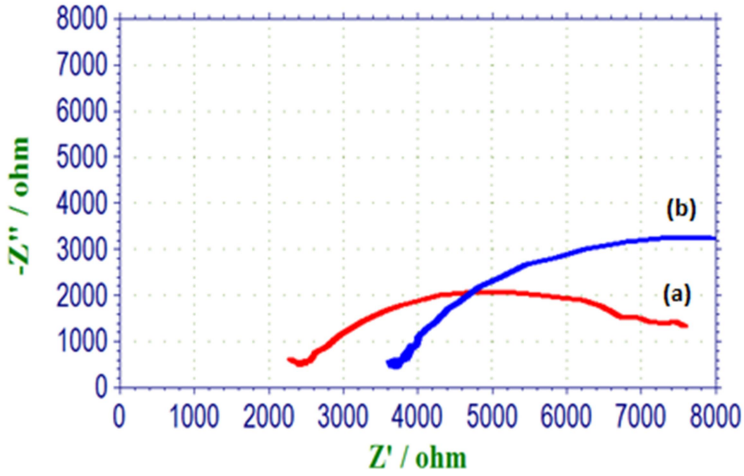

Figure 2: AC impedance spectra of carbon steel immersed in to SCP in the absence and presence of MPIMB inhibitor (Nyquist plots)
(a) Mild steel in SCP without inhibitor
(b) Mild steel in SCP with 60 ppm of MPIMB

Table 3: Electrochemical impedence parameters from Nyquist plots for the corrosion of mild steel for MPIMB in SCP

Systems	Nyquist plot		Bode plot
	R_t Ω cm^2	C_{dl} F cm^{-2}	Impedance Lg (Z ohm^{-1})
SCP	516	6.13×10^{-3}	0.500
SCP + 250 ppm MPIMB	593	4.66×10^{-3}	0.509

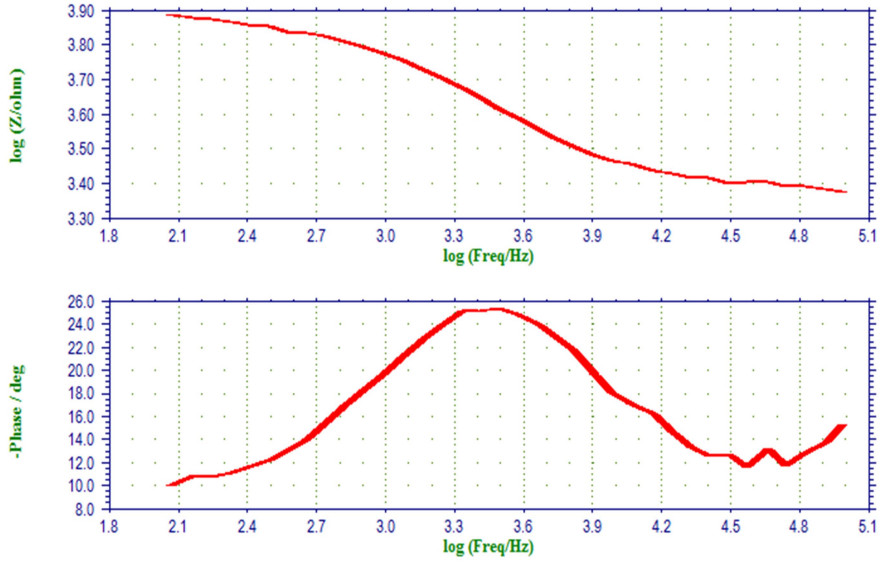

Figure 3a: AC impedance spectra of mild steel immersed in SCP (Bode Plot)

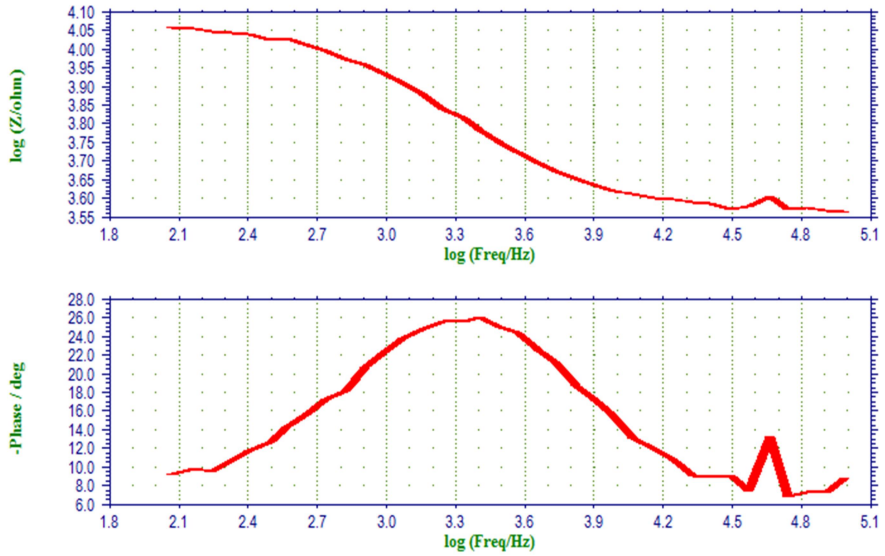

Figure 3b: AC impedance spectra of mild steel immersed in SCP with 250 ppm of MPIMB (Bode Plot)

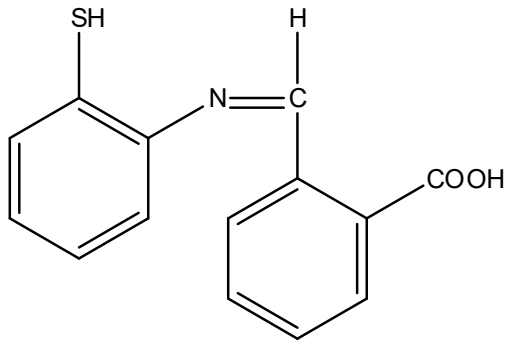

Figure 4: Structure of 2-[(2-mercapto-phenylimino) methyl] benzoic acid

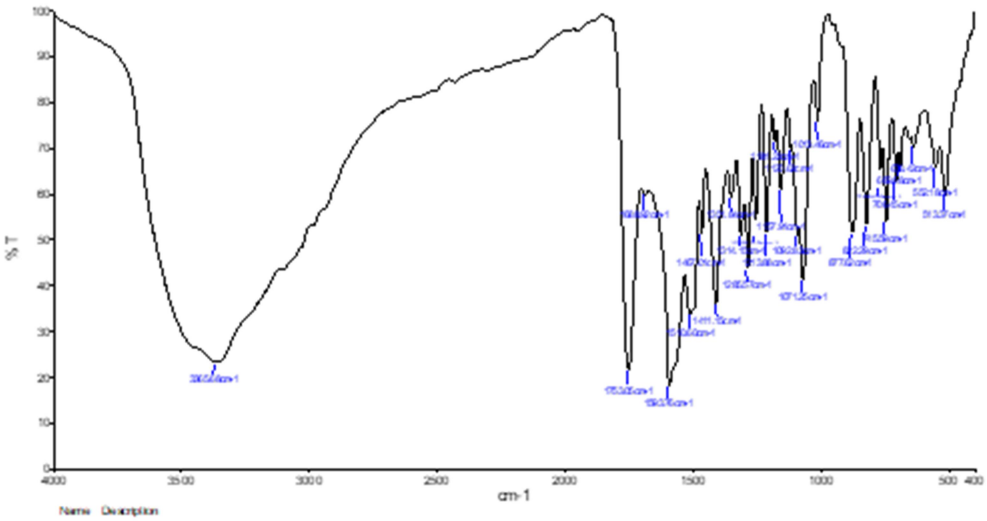

Figure 5a: FTIR Spectrum of Pure MPIMB

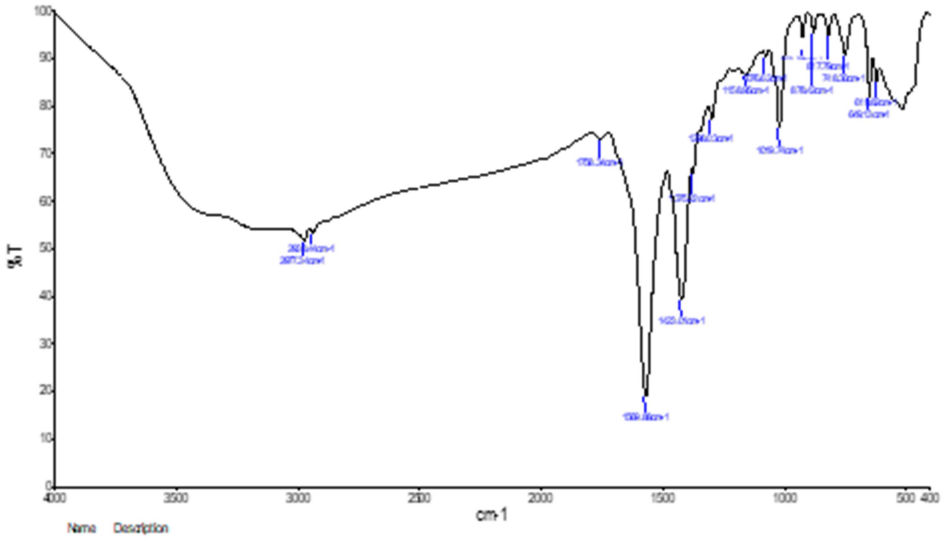

Figure 5b: FTIR spectrum of film formed on carbon steel surface after immersion in an aqueous solution containing SCP+ 250 ppm of MPIMB

Table 4: IR values of Pure MPIMB and film formed over the mild steel surface is obtained from IR Spectra

Functional Group	Pure MPIMB Compound (Peak Appears At) (cm^{-1})	The Protective film consists of Fe^{2+} -MPIMB (cm^{-1})
C=O	1688.92	1569.88
OH	3365.68	2977.34
C=N	1593.76	1569.88
SH	1013.46	1019.74
C=S	1157.91	1158.95
C=C	1285.57	1298.03

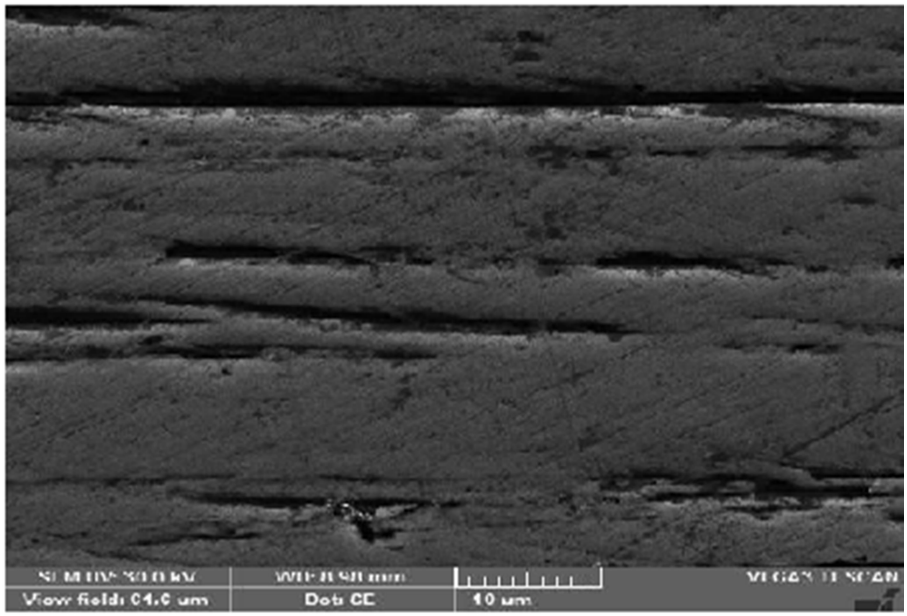

Figure 6a: SEM image of polished mild steel specimen before immersion in SCP (control)

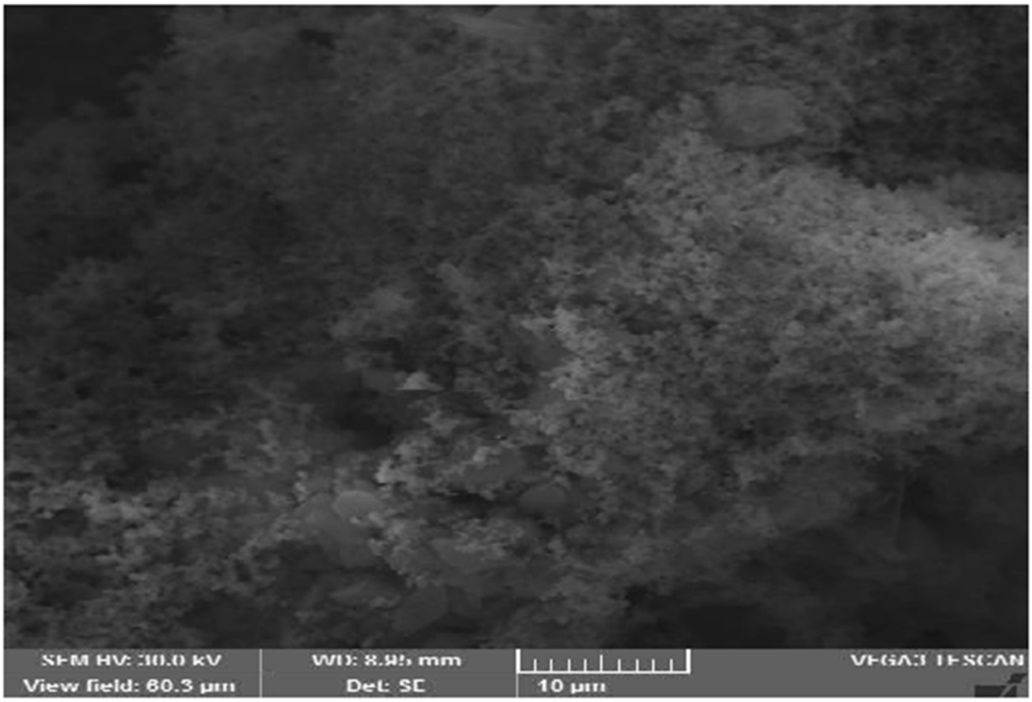

Figure 6b: SEM image of mild steel specimen after immersion in SCP (blank)

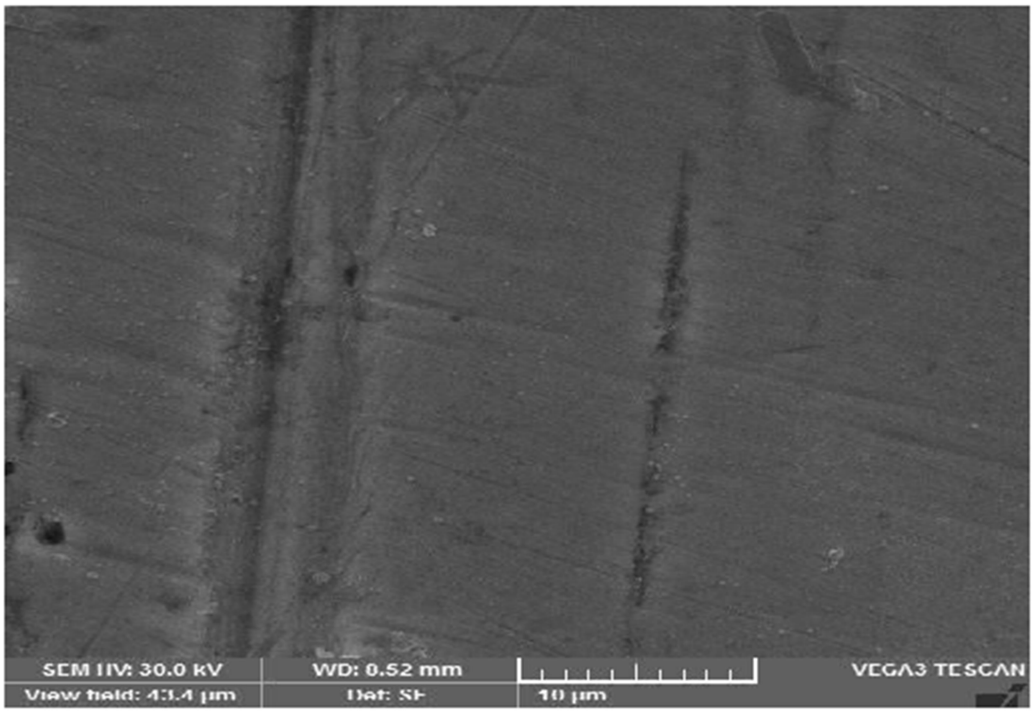

Figure 6c: SEM image of polished mild steel specimen after immersion in SCP in the presence of 250 ppm of MPIMB.

DISCUSSION

Analysis of results of weight loss method

It is observed that 250 ppm of MPIMB offers 90% of inhibition efficiency. It is observed from **Table 1** that MPIMB shows some inhibition efficiency. 250 ppm of MPIMB has 90% IE. As the concentration of MPIMB increases, the IE increases. This is due to an increase of surface coverage at higher concentrations of the inhibitor which retards the dissolution of carbon steel. The electron-donating properties of nitrogen and sulfur atoms along with delocalized π-electrons can be attributed to higher inhibition efficiencies. This surveillance is in good agreement with the results reported by many researchers **[19-20]**.

Analysis of results of potentiodynamic polarization study

When mild steel was immersed in an aqueous solution containing SCP the corrosion potential was - 508 mV vs SCE. When MPIMB (250 ppm) was added to the above system, the corrosion potential shifted to the positive side - 470 mV vs SCE. This indicates that the protective film is formed on the anodic sites of the carbon steel surface. This film controls the anodic reaction of carbon steel dissolution by forming Fe^{2+}-MPIMB complex on the anodic sites of the mild steel surface **[21-22]**. Further, the LPR value increases from 1740 ohm cm^2 to 1783 ohm cm^2, the corrosion current decreases from 2.443×10^{-7} A/cm^2 to 2.987×10^{-7} A/cm^2. Thus polarization study confirms the formation of a protective film on the carbon steel surface.

Analysis of results of alternating current impedance spectra

It is observed that when the inhibitor (250 ppm of MPIMB) is added, the charge transfer resistance (R_t) increases from 516 Ω cm^2 to 593 Ω cm^2. The C_{dl} value decreases from 6.13×10^{-3} F cm^{-2} to 4.66×10^{-4} F cm^{-2}. The impedance value [log (z/ohm)] increases from 0.500 to 0.509 **[23-24]**. These results lead to the conclusion that a protective film is formed on the carbon steel surface. Further, the phase angle increases from 25 to $26^{o.}$

Analysis of FTIR spectra

The C=O stretching frequency appears at 1688.92 cm^{-1}. The peak due to C=N appears at 1593.76 cm^{-1}. The peak appears at 3365.68 cm^{-1} due to OH stretching frequency. The SH stretching frequency appears at 1013.46 cm^{-1}. The C=S stretching frequency appears at 1157.91 cm^{-1}. The peak due to aromatic C=C appears at 1285.57 cm^{-1}. The C=O stretching has shifted from 1688.92 cm^{-1} to 1569.88 cm^{-1}. The C=N stretching frequency has shifted from 1593.76 cm^{-1} 1596.88 cm^{-1}. The OH

stretching frequency has shifted from 3365.68 cm^{-1} to 2977.34 cm^{-1}. The SH stretching frequency has shifted from 1013.46 cm^{-1} to 1019.74 $cm^{-}1$. The C=S stretching frequency has shifted from 1157.91 cm^{-1} to 1158.95 cm^{-1}. The peak due to aromatic C=C has shifted from 1285.57 cm^{-1} to 1298.03 cm^{-1} **[25-29]**. This observation suggests that MPIMB has coordinated with Fe^{2+} through the sulphur atom and nitrogen atom resulting in the formation of Fe^{2+}-MPIMB complex on the anodic sites of the mild steel surface. Thus the FTIR spectral study leads to the conclusion that the protective film consists of Fe^{2+}-MPIMB.

Surface analysis of mild steel by SEM

The SEM images of smooth mild steel surface in **Figure 6a** indicate the absence of any corrosion inhibitor formed on the mild steel surface **[30-31]**. **Figure 6b** SEM image of rough mild steel surface which indicate the highly corroded area. The **Figure 6c** SEM image of mild steel surface in presence of inhibitor is less corroded surface and smooth mild steel surface which is due to the strong adsorption of the corrosion inhibitor on the carbon steel surface and suppress the corrosion process.

However, in the presence of an inhibitor (250 ppm MPIMB), the rate of corrosion is slowed, as evidenced by the reduction in corroded areas. Due to the production of the insoluble complex on the mild steel surface, the mild steel surface is almost corrosion-free. The smoothness of the mild steel specimen is nearly identical to that of the polished mild steel surface **[32]**. In the presence of 250 ppm of MPIMB, the surface is covered by a thin layer of inhibitor which effectively controls the dissolution of mild steel immersed in SCP with 250 ppm of MPIMB. Thus it is revealed that the inhibitor has increased the efficiency of adsorption at the mild steel/solution interface and thus the inhibitors tend to reduce metallic surface destruction **[33]**.

CONCLUSION

In the current study, the compound 2-[(2-mercapto-phenylimino) methyl] benzoic acid has been used as a corrosion inhibitor. In an aqueous solution containing SCP, this inhibitor has been utilized as a corrosion inhibitor to keep mild steel from corroding. The results of the weight-loss method, polarisation studies, AC impedance measurements, and surface examination techniques such as FTIR spectroscopy and scanning electron spectroscopy are used to determine the mechanistic elements of corrosion inhibition. The rate of corrosion is

decreased with the increasing addition of organic compounds, probably due to progressive adsorption of the inhibitor on the metal surface. The maximum inhibition efficiency was found to be 84%.

The present study leads to the following conclusions

- The inhibitor exhibit good corrosion inhibition efficiency in controlling the corrosion of mild steel corrosion in an aqueous solution containing SCP^-.
- Polarization study shows that the effective inhibitor systems function as anodic inhibitors controlling the anodic reaction predominantly.
- The weight loss technique shows an inhibition efficiency 84%.
- Electrochemical impedance measurements indicate that an increase in the charge transfer resistance ($_{Rt}$), decrease the double-layer capacitance ($_{Cdl}$) and corrosion current ($_{Icorr}$) values owing to the increased thickness of the adsorbed layer.
- FTIR spectra reveal that the protective film consists of Fe^{2+}-inhibitor complex
- SEM micrographs show the smoothness of carbon steel surfaces like polished mild steel.

Conflict of Interest

The authors declare that there is no conflict of interest regarding the publication of this article.

REFERENCES

[1] Nagalakshmi R, Rajendran S, Sathiyabama J, Pandiarajan M, Lydia Christy. corrosion resistance of al in simulated concrete pore solution in the presence of curcumin extract corrosion resistance of commercial aluminium in simulated concrete pore solution in presence of curcumin extract. J. Eur. Chem. Bull, 2012;1(17): 238.

[2] Rajendran S, Sridevi S P, Antony N, John Amalraj A, Sundaravadivelu N. Corrosion behaviour of carbon steel in polyvinyl alcohol. Anti.Corros. Methods. Mater. 2005;52: 102.

[3] Anandan A, Rajendran S, Sathiyabama J and Sathiyara D. Influence of some tablets on corrosion resistance of orthodontic wire made of SS 316L alloy in artificial saliva. Int. J. Corros. Scale Inhib. 2017; 6(2):132–141.

[4] Khadraoui A, Khelifa A, Hachama K, Mehdaoui R, Thymus algeriensis extract as a new eco-friendly corrosion inhibitor for 2024 aluminium

alloy in 1 M HCl medium. J. Mol. Liq. 2016; 214(2): 93–7.

[5] Gunavathy N, Murugavel SC. Corrosion inhibition of mild steel in acid medium using MUSA acuminata flower extract. J. Environ Nanotechnol. 2013; 2(4): 45–50.

[6] El Bribri A, Tabyaoui M, Tabyaoui B, El Attari H, Bentiss F. The use of Euphorbia falcata extract as eco-friendly corrosion inhibitor of carbon steel in hydrochloric acid solution. Mater. Chem Phys. 2013;141(1): 1–7.

[7] Mourya P, Banerjee S, Singh MM. Corrosion inhibition of mild steel in acidic solution by Tagetes erecta (Marigold flower) extract as a green inhibitor. Corros Sci. 2014; 85(3): 52–63.

[8] Li L, Zhang X, Lei J, He J, Zhang S, Pan F. Adsorption and corrosion inhibition of Osmanthus fragran leaves extract on carbon steel. Corros Sci. 2012; 63: 82–90.

[9] Rajendran A. Isolation, characterization, pharmacological and corrosion inhibition studies of flavonoids obtained from Nerium oleander and Tecoma stans. Int. J. Pharmtech Res. 2011; 3 (2): 1–13.

[10] Mohammed A.El-Hashemy, AmalSallam. The inhibitive action of *Calendula officinalis* flower heads extract for mild steel corrosion in 1 M HCl solution, J. Mat. Research and Technol. 2020; 9(6):13509–13523.

[11] Gunavathy S. Murugavel S. Corrosion inhibition studies of mild steel in acid medium using musa acuminate fruit peel extract. E-Journal of Chemistry. 2012; 9(1): 487-495.

[12] Mohammed Al Hashemy, Amal Sallam. The inhibitive action of *calendula officinalis* flower heads extract for mild steel corrosion in 1 M HCl solution. Journal of Materials Research and Technology. 2020; 9(6): 13509-13513.

[13] Aprael S, Yaro Rafal K, Wael A, Anees A. Khadom, Reaction Kinetics of Corrosion of Mild Steel in Phosphoric Acid. Journal of the University of Chemical Technology

and Metallurgy. 2010; 45(4): 443-448.

[14] Syed Abuthahir SS, Jamal Abdul Nasser A, Rajendran S. Inhibition effect of copper complex of 1-(8-Hydroxy quinolin-2yl-methyl) thiourea on the corrosion of mild steel in Sodium Chloride solution. The Open Material Science Journal. 2014; 8: 71-80.

[15] Nazeera Banu VR, Rajendran S, Syed Abuthahir SS. Corrosion Inhibition by Self-assembling Nano films of Tween 60 on Mild steel surface. International Journal of Chemical Concepts. 2017; 3(1): 161-173.

[16] Karthik Kumar K, Selvaraj SK, Pandeeswaran M, Syed Abuthahir SS, John Amalraj A. Synergistic Corrosion Inhibition Effect of Carbon Steel in Sea Water by Hydroxy Proline - Zn^{2+} System. International Journal of Advanced Chemical Science and Applications. 2015; 3(4): 54-59.

[17] Fabrizio Zucchi, Ibrahim Hashi Omar, Plant extracts as corrosion inhibitors of mild steel in HCl solutions. Surface Technology. 1985; 24(4): 391- 399.

[18] Samsath Begum A, Jamal Abdul Nasser A, Mohamed Kasim Sheit H, Varusai Mohamed M. Abrus precatorius leaf aqueous extract as a corrosion inhibitor on Mild steel in 1.0 M HCl solution. International Journal of basic and applied research. 2019; 9(2): 438-450.

[19] Tuama RJ, Al-Dokheily ME, Khalaf MN. Recycling and evaluation of poly (ethylene terephthalate) waste as effective corrosion inhibitors for C-steel material in acidic media. Int. J. Corros. Scale Inhib. 2020; 9(2): 427–445.

[20] Jeeva PA, Mali GS, Dinakaran R, Mohanam K, Karthikeyan S. The influence of Co-Amoxiclav on the corrosion inhibition of mild steel in 1 N hydrochloric acid solution. Int. J. Corros. Scale Inhib. 2019; 8(1): 1–12.

[21] Shanthy P, Thangakani JA, Karthika S, Joycee SC, Rajendran S, Jeyasundari J. Corrosion inhibition by an aqueous extract of Ervatamia divaricate. Int. J. Corros. Scale Inhib. 2021; 10(1): 331–348.

[22] Barrahi M, Elhartiti H, A. El Mostaphi, Chahboun N, Saadouni M, Salghi R, Zarrouk A, Ouhssine

M. Corrosion inhibition of mild steel by Fennel seeds (Foeniculum) vulgare Mill) essential oil in 1 M hydrochloric acid solution. Int. J. Corros. Scale Inhib. 2019; 8(4): 937–953.

[23] Mahalakshmi P, Rajendran S, Nandhini G, Joycee SC, Vijaya N, Umasankareswari T, Renuga Devi N. Inhibition of corrosion of mild steel in sea water by an aqueous extract of turmeric powder. Int. J. Corros. Scale Inhib. 2020; 9(2): 706–725.

[24] Ikhmal WMKWM,. Yasmin MYN, Mari MFF,. Syaizwadi SM, Rafizah WAW, Sabri MGM, Zahid, BM. Evaluating the performance of Andrographis paniculata leaves extract as additive for corrosion protection of stainless steel 316L in sea water. Int. J. Corros. Scale Inhib. 2020; 9(1): 118–133.

[25] Grace Baby A, Rajendran S, Johnsirani V, Al-Hashem A, Karthiga N, Nivetha P. Influence of zinc sulphate on the corrosion resistance of L80 alloy immersed in sea water in the absence and presence of sodium potassium tartrate and trisodium citrate. Int. J. Corros. Scale Inhib. 2020; 9(3): 979–999.

[26] Rajendran S, Srinivasan R, Dorothy R, Umasankareswari T, Al-Hashem A. Green solution to corrosion problems – at a glance. Int. J. Corros. Scale Inhib. 2019; 8(3): 437–479.

[27] Peter A, Sharma S.K. Use of Azadirachta indica (AZI) as green corrosion inhibitor against mild steel in acidic medium: anti-corrosive efficacy and adsorptive behavior. Int. J. Corros. Scale Inhib. 2017; 6(2): 112–131.

[28] Dehghani A, Bahlakeh G, Ramezanzadeh B, Ramezanzadeh M. Potential role of a novel green eco-friendly inhibitor in corrosion inhibition of mild steel in HCl solution: Detailed macro/micro-scale experimental and computational explorations. Constr. Build. Mater. 2020; 245: 118464.

[29] Kıcır N, Tansu˘ G, Erbil M, Tüken T. Investigation of ammonium (2, 4-dimethylphenyl)-dithiocarbamateas a new effective corrosion inhibitor for mild steel. Corros. Sci. 2016; 105: 88–99.

[30] Verma C, Ebenso EE, Bahadur I,.

Quraishi MA, An overview on plant extracts as environmental sustainable and green corrosion inhibitors for metals and alloys in aggressive corrosive media. J. Mol. Liq. 2018; 266: 577–590.

[31] Karthikeyan S, Syed Abuthahir SS, Samsath Begum A, Vijaya K. Corrosion Inhibition of Mild Steel in 0.5 M H2SO4 Solution by Plant Extract of Annona squamosal. Asian Journal of Chemistry. 2021; 33(9): 2219-2228.

[32] Rajendran S, Apparao BV, Palaniswamy N. Corrosion and corrosion inhibition of delta-steel in acid chloride solutions containing pyrazole compound. Bulletin of Electrochemistry. 1996; 12:15.

[33] Behpour M, Ghoreishi SM, Soltani N, Salavati-Niasari N, Hamadanian M, Gandomi A. Inhibiting Effect of Dioctyl Phthalate on the Corrosion of Mild Steel in 1.0 M Hydrochloric Acid Solution. Corros. Sci., 2008; 50: 2172-2181.